Multinuclear NMR Study of the Conformational Changes in Me*p*dG and dG*p*Me upon Interaction with Mg^{2+}, Zn^{2+} and Hg^{2+} Ions Reveals the Strengthening of the Anomeric Effect by Soft M^{2+} Ions

Matjaž Polak[a] and Janez Plavec*[a]

Keywords: Nucleotides / Conformation analysis / NMR spectroscopy / Pseudorotational equilibrium / Anomeric effect

A conformational study is reported on 2′-deoxyguanosine 5′-methylmonophosphate [Me*p*dG (**1**)] and 2′-deoxyguanosine 3′-methylmonophosphate [dG*p*Me (**2**)] and their interactions with Mg^{2+}, Zn^{2+} and Hg^{2+} ions. The conformation of Me*p*dG (**1**) and dG*p*Me (**2**) in D_2O solution was inferred from vicinal proton-proton, proton-phosphorus and carbon-phosphorus NMR coupling constants and nuclear Overhauser effects (NOE). The chemical shift changes showed that hard Mg^{2+} ions interact preferentially with the phosphate oxygen atoms in Me*p*dG (**1**), whereas in the case of dG*p*Me (**2**) the interaction with the phosphate oxygen atoms competes with the interaction to the C6=O carbonyl group. Softer Zn^{2+} and Hg^{2+} ions were found to show strong binding affinity towards N7 in both Me*p*dG (**1**) and dG*p*Me (**2**). Analysis of *J* coupling constants and NOEs measured as a function of metal ion concentration revealed that: (i) N $\rightleftarrows$ S pseudorotational equilibria are biased towards C2′-*endo* pseudorotamers in M^{2+}-free Me*p*dG (**1**) and dG*p*Me (**2**) by 68% and 75% at 298K, respectively. Titration of Me*p*dG (**1**) and dG*p*Me (**2**) with Mg^{2+} ions caused no observable changes in N $\rightleftarrows$ S pseudorotational equilibrium, whereas the interactions of Zn^{2+} and Hg^{2+} ions with N7 resulted in the shift towards N-type pseudorotamers which can be explained by the strengthening of the anomeric effect as softer metal ions bind to N7 and make the imidazole moiety less electron-rich. (ii) The binding of divalent metal ions to Me*p*dG (**1**) and dG*p*Me (**2**) causes a shift of the *syn* $\rightleftarrows$ *anti* equilibrium towards *anti*, which is larger for softer Zn^{2+} than for harder Mg^{2+} ions. (iii) The conformational equilibrium across the C4′–C5′ bond (γ torsion) in dG*p*Me (**2**) is not affected by the increased concentration of M^{2+} ions. (iv) β^t conformers are preferred by ca. 77% in aqueous solution of Me*p*dG (**1**) and only small changes of ca. 1 percentage point in β^t population have been found upon metal ion binding to Me*p*dG (**1**). (v) The two-state $\varepsilon^t \rightleftarrows \varepsilon^-$ conformational equilibrium is biased towards ε^t rotamers by 63.5% in dG*p*Me (**2**). Interaction of hard Mg^{2+} and softer Zn^{2+} or Hg^{2+} ions with dG*p*Me (**2**) resulted in the minor increase (< 3 percentage points) in the population of ε^t conformers.

Introduction

The structure and function of nucleic acids depend on metal ions. A knowledge of the effects of metal species on DNA structures is important in understanding the natural role of metal species.[1] Monovalent alkaline cations and divalent alkaline-earth metal cations interact preferentially with the phosphate groups, which stabilizes the DNA double duplex by neutralizing the negatively charged sugar-phosphate backbone, and to a lesser extent with the bases.[2] Interactions of divalent cations with nucleobases are involved in many biophysical processes and can cause polarization of nucleobases associated with the stabilization of certain hydrogen bonds between A=T and G≡C Watson-Crick base pairs as well as Hoogsteen base pairs in triplex DNA. Little is, however, known in the literature about how the interaction of metal ions with particular nucleotide in oligomeric fragment affects its conformation and how this local conformational change is transmitted into reorganization of the three-dimensional structure. In order to study local conformational changes induced by metal ions we have prepared two simple mononucleotide models of DNA, Me*p*dG (**1**) and dG*p*Me (**2**), which consist of all the essential structural elements of DNA to which metal ions can interact: β-D-2′-deoxyribofuranose, the phosphodiester fragment and the heterocyclic moiety.

The phosphodiester groups in Me*p*dG (**1**) and dG*p*Me (**2**) carry one negative charge at neutral pH and are expected not to overestimate the effect of electrostatic association of metal ions and a nucleotide on the structural change of nucleic acids. With the use of high-field multinuclear ^{1}H-, ^{13}C-, ^{15}N- and ^{31}P-NMR spectroscopy we were able to identify the binding sites for the individual metal ions on Me*p*dG (**1**) and dG*p*Me (**2**), and to examine the conformational changes along the glycosyl bond (*syn* $\rightleftarrows$ *anti* equilibrium, torsion angle χ), pseudorotational equilibrium of sugar moiety between North- and South-type conformers, reorientation along C4′−C5′ bond (torsion angle γ) and the conformational equilibria along phosphodiester fragments with torsion angles β[P−O5′−C5′−C4′] and ε[C4′−C3′−O3′−P] in Me*p*dG (**1**) and dG*p*Me (**2**), respectively.

According to the pseudorotation concept[3] the furanosyl ring in nucleosides and nucleotides[4,5] is involved in interconversions of puckered envelope and twist forms. The puckering mode can be defined by Altona−Sundaralingam parameters[4,5] which are the phase angle of pseudorotation (*P*) and the maximum puckering amplitude (Ψ_m). *P* defines

[a] National Institute of Chemistry,
Hajdrihova 19, SI-1115 Ljubljana, Slovenia
Fax: (internat.) + 386-61/125-9244
E-mail: janez.plavec@ki.si

  1434−1948/99/0303−0547 $ 17.50+.50/0

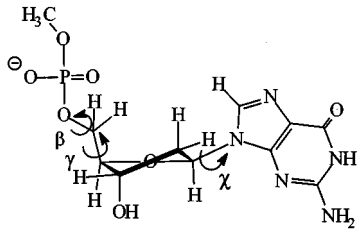

MepdG (**1**)

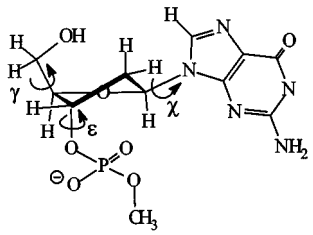

dGpMe (**2**)

Figure 1. Structural formula of MepdG (**1**) and dGpMe (**2**)

the part of the ring which is most puckered and Ψ_m indicates the extent of the puckering. In a survey of X-ray crystal structures[6] of nucleosides and nucleotides sugar moieties were found in both North (N) and South (S) conformations. The former range ($0° < P < 36°$) is centered around $P = 18°$ (C3′-*endo*), whereas the latter ($144° < P < 180°$) is centered around $P = 162°$ (C2′-*endo*). The values of Ψ_m were found in a range from 30° to 46°.[6] A large collection of NMR data is consistent with the conformational equilibrium between two distinctly identifiable N and S conformations which are dynamically interconverting in solution. Two-state N $\rightleftharpoons$ S pseudrotational equilibrium is controlled by the competing anomeric and *gauche* effects.[7] The 3′-OH or 3′-phosphate groups in 2′-deoxynucleos(t)ides drive the N $\rightleftharpoons$ S equilibrium towards S-type conformation through the tendency to adopt a *gauche* orientation of the [O4′−C4′−C3′−O3′] torsion angle.[7,8] The heterocyclic bases are involved in the anomeric effect which results in the energetic preference of N-type (pseudoaxial nucleobase) over S-type (pseudoequatorial nucleobase) conformation in terms of the anomeric effect alone. The anomeric effect in nucleosides involves the interaction between the non-bonded lone pairs of O4′ and the antibonding σ* orbital of the glycosyl bond (*i.e.* $n_{O4'} \rightarrow \sigma^*_{C1'\text{-}N}$ orbital overlap) and its strength is closely related to the electronic nature of the aglycone.[7,9−15] The protonation of the nucleobase facilitates the $n_{O4'} \rightarrow \sigma^*_{C1'\text{-}N}$ interactions, thereby resulting in the increased population of N-type conformers.[12−14,16] We have already shown in our preliminary study on the conformational changes induced by metal ion binding to 2′-dG that Zn^{2+} and Hg^{2+} bind to N7 and shift the N $\rightleftharpoons$ S pseudorotational equilibrium towards N by 0.8 percentage points ($R = 2.0$) and 4.1 percentage points ($R = 0.2$), respectively.[17] In the present study we have chosen three divalent metal ions (Mg^{2+}, Zn^{2+} and Hg^{2+}) which differ in their soft-hard nature and are known to have distinct binding modes to nucleic acids. Hard metal ions like Mg^{2+} are expected to bind to phosphate oxygen atoms in MepdG (**1**) and dGpMe (**2**), which would alter the strength of the [O4′−C4′−C3′−O3′] *gauche* effect in dGpMe (**2**) in particular and should change the population of S-type conformers in dGpMe (**2**). On the other hand, possible binding of Mg^{2+} to C6=O of guanine ring[18] would change the electron distribution in the purine moiety and thus specifically affect the N $\rightleftharpoons$ S pseudorotational equilibrium through the modulation of the anomeric effect. Soft metal ions like Hg^{2+} will bind to N7 of the guanine ring which is expected to increase the population of the N-type conformers due to the strengthening of the anomeric effect. It is, however, hard to predict how the increase in the steric bulk due to soft metal ion binding to N7 of MepdG (**1**) and dGpMe (**2**) would additionally shift the N $\rightleftharpoons$ S pseudorotational equilibrium towards S. Zn^{2+} is expected to have affinities for both the nucleobase and the phosphate groups and is therefore expected to change both the anomeric effect as well as the strength of the [O4′−C4′−C3′−O3′] *gauche* effect.

Results and Discussion

Binding Sites

The affinity of metal ions towards the specific electron-rich sites in MepdG (**1**) and dGpMe (**2**) has been studied by monitoring the changes in their ^1H, ^{13}C, ^{15}N and ^{31}P NMR chemical shifts as the concentration of Mg^{2+}, Zn^{2+} and Hg^{2+} ions was gradually increased to 0.1, 0.2, 0.5, 1.0 and 2.0 molar equivalents. Titration of MepdG (**1**) and dGpMe (**2**) with two molar equivalents of Mg^{2+} ions resulted in a very small chemical shift change of a few ppb for the H8 signal (Figure 2), which indicates the absence, or possibly very weak interaction of Mg^{2+} with N7 of the guanine moiety.[19] In addition, the small ^1H-, ^{13}C- and ^{15}N-NMR$\Delta\delta$ values reported in Table 1 for MepdG (**1**) indicate a very weak interaction of Mg^{2+} ions with the pentofuranose moiety, phosphodiester or the heterocyclic ring in MepdG (**1**). On the other hand, the addition of two molar equivalents of Mg^{2+} ions to dGpMe (**2**) caused a downfield shift of 0.143 ppm for the C6 signal, which suggests an interaction of Mg^{2+} ions with the C6=O carbonyl oxygen atom under neutral pH. We have furthermore detected changes of 0.4 Hz in $^2J_{PC5'}$ and $^2J_{PCH3}$ coupling constants for MepdG (**1**), which indicate that Mg^{2+} ions interact with oxygen atoms of the phosphate group and possibly influence rotamer population across β (vide infra).

Titration of MepdG (**1**) and dGpMe (**2**) with up to two molar equivalents of Zn^{2+} ions resulted in the progressive downfield shift of the H8 signal (Figure 2). The affinity of Zn^{2+} aqua ions to bind to N7 of the nucleobase[20] has been independently confirmed with ^{13}C- and ^{15}N-NMR data (Table 1). The ^{31}P chemical shifts of MepdG (**1**) and

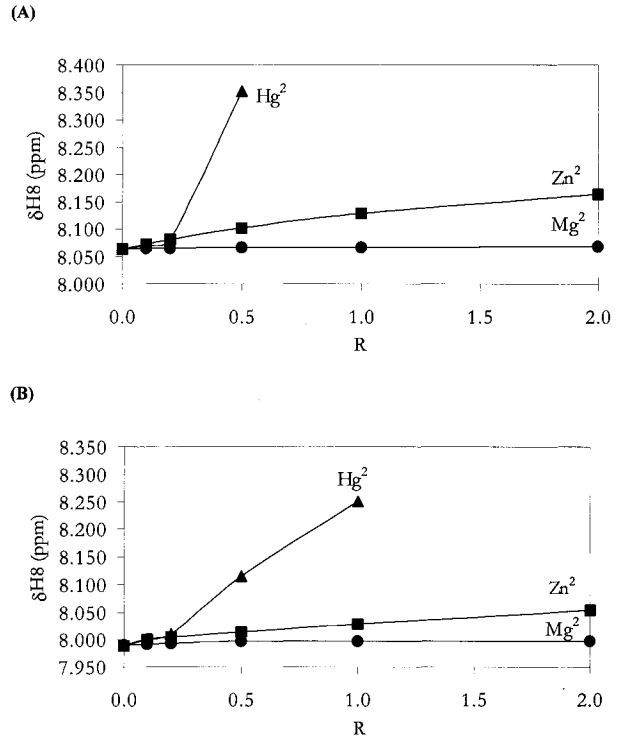

Figure 2. Changes of H8 chemical shifts as a function of increasing metal ion concentration in D_2O solution of Me*p*dG (**1**) (panel A) and dG*p*Me (**2**) (panel B); in the case of Hg^{2+} ions the precipitation precludes the extraction of NMR chemical shifts above R = $[M^{2+}]$/[nucleotide] = 1.0

dG*p*Me (**2**) moved upfield by 0.095 ppm and 0.018 ppm, respectively, upon addition of two molar equivalents of Zn^{2+} ions which suggests that the coordinative interaction between Zn^{2+} and phosphate oxygen atoms is negligible. It is noteworthy that chelation[21−26] of N7 and α-PO_4 monoester in 6-oxopurine nucleotide monophosphates by Pt^{2+} resulted in a downfield Δδ(^{31}P) shift of 3.5 ppm.[21] The ^{31}P chemical shifts are, however, sensitive[27] to bond angle changes, conformational changes along α and ζ and environmental effects, and are therefore difficult to correlate with the strength of binding of metal ions with phosphate groups. The addition of more than 0.2 molar equivalents of Hg^{2+} ions to the aqueous solutions of Me*p*dG (**1**) or dG*p*Me (**2**) resulted in the broadening of ^{1}H-NMR signals probably due to macrochelation, which was followed by precipitation after the addition of one molar equivalent of Hg^{2+} ions. The downfield shifts of H8 resonances upon addition of Hg^{2+} ions were much larger than in the case of Zn^{2+} (Figure 2) which is in agreement with the softer nature of Hg^{2+} ions and indicates strong binding affinity towards N7 (Table 1).

North ⟺ South Pseudorotational Equilibrium

The analysis of the solution conformation of the 2′-deoxy-β-D-ribofuranosyl moiety in Me*p*dG (**1**) and dG*p*Me (**2**) is based on five ($^3J_{1'2'}$, $^3J_{1'2''}$, $^3J_{2'3'}$, $^3J_{2''3'}$ and $^3J_{3'4'}$) proton-proton coupling constants (Table 2) which have been interpreted in terms of a two-state N ⟺ S pseudorotational equilibrium, as is normal for 2′-deoxyribose rings (see Experimental Section).[4,5,29−31] The titration of both Me*p*dG (**1**) and dG*p*Me (**2**) with Mg^{2+} ions caused no observable changes in $^3J_{HH}$ coupling constants (Table 2). In the case of Zn^{2+} and Hg^{2+} ions, we observed considerable changes in $^3J_{HH}$ coupling constants, which indicated that the N ⟺ S pseudorotational equilibrium were perturbed

Table 1. The comparative effects of Mg^{2+}, Zn^{2+} and Hg^{2+} ions on the ^{1}H-, ^{13}C-, ^{31}P- and ^{15}N-NMR chemical shifts[a] of Me*p*dG (**1**) and dG*p*Me (**2**)

	Me*p*dG (**1**)				dG*p*Me (**2**)			
	M^{2+}-free	Mg^{2+} (R = 2.0)	Zn^{2+} (R = 2.0)	Hg^{2+} (R = 0.2)	M^{2+}-free	Mg^{2+} (R = 2.0)	Zn^{2+} (R = 2.0)	Hg^{2+} (R = 0.2)
H8	8.064	0.003	0.100	0.016	7.990	0.008	0.064	0.021
H1′	6.333	−0.002	0.022	0.005	6.344	−0.001	0.007	0.002
H2′	2.847	−0.008	−0.030	−0.010	2.875	0.000	−0.001	0.001
H2″	2.542	0.002	0.031	0.040	2.678	0.004	0.014	0.008
H3′	4.717	−0.003	0.011	−0.010	4.937	0.001	0.002	0.000
H4′	4.246	−0.001	0.013	0.013	4.320	−0.001	−0.001	−0.012
H5′	4.040	0.000	0.019	0.014	3.860	0.000	0.004	−0.009
H5″					3.805	0.000	0.004	−0.010
C6	161.846	0.005	−0.107	−0.032	161.912	0.143	−0.040	−
C8	140.409	0.062	0.482	0.128	140.826	0.005	0.323	0.072
C4′	88.550	0.016	0.072	0.097	89.218	−0.025	0.001	−0.003
C1′	86.475	0.040	0.232	0.176	87.055	−0.010	0.064	0.013
C3′	74.113	0.014	−0.180	0.039	78.559	−0.043	−0.137	−0.034
C5′	67.981	0.048	−0.126	0.053	64.451	−0.002	−0.047	−0.008
Me	55.620	0.054	0.062	0.078	55.758	0.030	0.055	0.018
C2′	41.364	0.085	0.317	0.115	40.687	0.001	0.045	0.003
P	2.342	−0.064	−0.095	−0.020	1.593	−0.037	−0.018	−0.023
N7	−145.3	−0.6	−8.4	−1.5	−146.4	0.0	−4.2	−0.5
N9	−207.2	0.0	0.9	−	−209.1	0.5	1.0	−

[a] Chemical shifts for free Me*p*dG (**1**) and dG*p*Me (**2**), and Δδ [= $\delta_M{}^{2+}$(R) − δ_{free}] values for each of the metal ions are given in ppm. The positive Δδ value indicates that the particular resonance is shifted downfield upon addition of the metal ion. ^{1}H- and ^{13}C-NMR chemical shifts are referenced relative to trimethylsilylpropionic acid.

Table 2. Experimental J_{HH}, J_{HP} and J_{CP} coupling constants as a function of metal ion concentration in aqueous solution of Me*p*dG (**1**) and dG*p*Me (**2**) at 298 K[a]

Metal	Me*p*dG (**1**)				dG*p*Me (**2**)			
	M^{2+}-free	Mg^{2+}	Zn^{2+}	Hg^{2+}	M^{2+}-free	Mg^{2+}	Zn^{2+}	Hg^{2+}
R	0.0	2.0	2.0	0.2	0.0	2.0	2.0	0.2
$^3J_{H1'H2'}$	7.4	7.4	6.7	7.2	8.1	8.1	7.7	7.9
$^3J_{H1'H2''}$	6.4	6.5	6.5	6.4	6.1	6.1	6.3	6.2
$^3J_{H2'H3'}$	6.2	6.2	6.2	6.3	6.1	6.1	6.1	6.1
$^3J_{H2''H3'}$	3.6	3.7	4.0	3.6	2.8	2.8	3.0	2.9
$^3J_{H3'H4'}$	3.1	3.1	3.1	2.9	2.6	2.7	2.8	2.6
$^3J_{H4'H5'}$	3.9	3.9	3.5	3.9	3.4	3.4	3.4	3.4
$^3J_{H4'H5''}$					4.5	4.5	4.6	4.6
$^3J_{H2'P3'}$					0.8	0.8	0.7	0.8
$^3J_{H3'P3'}$					7.2	7.2	7.1	7.2
$^3J_{H4'P5'}$	1.7	1.6	2.0	1.6				
$^3J_{H5'/5''P5'}$	5.0	5.0	4.9	5.0				
$^3J_{C2'P3'}$					3.5	3.5	3.3	3.2
$^3J_{C4'P3'}$					5.8	6.0	5.7	6.0
$^3J_{C4'P5'}$	8.6	8.5	8.7	8.5				
$^3J_{C5'P5'}$	5.5	5.1	5.4	5.2				
$^2J_{C3'P3'}$					5.3	5.2	5.1	4.9
$^2J_{CH3P3'}$					5.8	5.6	5.6	6.1
$^2J_{CH3P5'}$	6.1	5.7	5.9	5.8				

[a] Coupling constants are listed only at two limiting concentrations ($R = 0$ and $R = 2.0$ or 0.2), whereas they have been collected as a function of increasing R. The coupling constants at all concentrations of metal ions ($0.0 < R < 2.0$) have been used in the conformational analysis. The signals for H5′ and H5" were isochronous for Me*p*dG (**1**). $^2J_{2'2''}$ was 14.0 and 14.2 Hz for Me*p*dG (**1**) and dG*p*Me (**2**), respectively. $^2J_{5'5''}$ was 12.5 Hz for dG*p*Me (**2**). $^2J_{2'2''}$ and $^2J_{5'5''}$ did not change by increasing the concentration of metal ions.

as the softer metal ions interacted with Me*p*dG (**1**) and dG*p*Me (**2**).

In the elaboration of the experimental $^3J_{HH}$ coupling constants at various metal ion concentrations we have used the computer program PSEUROT,[31] which calculates the least-squares fit of the five parameters defining the two-state N $\rightleftharpoons$ S pseudorotational equilibrium (P_N, $\Psi_m{}^N$, P_S, $\Psi_m{}^S$ and x_S) to the set of experimental $^3J_{HH}$ coupling constants. Our analysis incorporated 30 (i.e. 6×5) $^3J_{HH}$ coupling constants in the case of Mg^{2+} and Zn^{2+} ions, 15 (i.e. 3×5) $^3J_{HH}$ coupling constants in the case of Hg^{2+} ions and five $^3J_{HH}$ coupling constants for metal-free aqueous solutions of Me*p*dG (**1**) and dG*p*Me (**2**). As $^3J_{HH}$ coupling constants in Me*p*dG (**1**) and dG*p*Me (**2**) indicated a bias of N $\rightleftharpoons$ S pseudorotational equilibrium towards S-type conformers, the maximum puckering amplitude of the minor N-type component ($\Psi_m{}^N$) was constrained in the iterative procedure to find the best fit between experimental and calculated coupling constants. All other parameters were freely optimized (see the Experimental Section for details). The final convergence resulted in the global minima for each metal ion data set with root-mean-square error below 0.3 Hz and the maximum discrepancy between experimental and calculated coupling constants (ΔJ_{max}) below 0.5 Hz. The results in Table 3 show that the geometry of the minor N conformer is characterized by C2′-*exo* puckering ($-32.1° < P_N < -22.0°$, $37.3° < \Psi_m{}^N < 38.2°$), whereas the major S conformer is characterized by C2′-*endo* puckering ($161.5° < P_S < 166.5°$, $37.3° < \Psi_m{}^S < 38.2°$). Two important conclusions can be drawn from the data in Table 3. First, the interaction of Me*p*dG (**1**) and dG*p*Me (**2**) with divalent metal ions results in only a minute variation in the geometry of the pseudorotamers in both N and S regions of conformational space. The differences in the pseudorotational parameters P and Ψ_m are certainly a matter of degree, not of kind. Second, the gradual increase in the concentration of metal ions has direct influence on the population of N- and S-type conformers in Me*p*dG (**1**) and dG*p*Me (**2**) (Figure 3). The largest shift of N $\rightleftharpoons$ S pseudorotational equilibrium towards N-type conformers was 5 percentage points upon addition of two molar equivalents of Zn^{2+} to Me*p*dG (**1**). The binding of metal ions to N7 makes the imidazole moiety less electron-rich which strengthens the anomeric effect of the heterocyclic nucleobase in Me*p*dG (**1**) and dG*p*Me (**2**). Note that the changes in the N $\rightleftharpoons$ S pseudorotational equilibrium are smaller than changes caused by N7 protonation.[12] The smaller drive towards N-type sugar conformation due to the interaction of divalent metal ions with N7 of guanine in Me*p*dG (**1**) and dG*p*Me (**2**) relative to that due to protonation could be explained by the solvation of the metal ions. Water molecules, which mediate M^{2+} interactions with nucleotides reduce the effect of the metal ion on the redistribution of electron density in guanine. The increase in the population of N-type conformers upon interaction with two molar equivalents of Zn^{2+} is larger for Me*p*dG (**1**) than for dG*p*Me (**2**). The interaction of Zn^{2+} with the 5′-phosphodiester in Me*p*dG (**1**) is not expected to affect the N $\rightleftharpoons$ S pseudorotational equilibrium directly. The N7-phosphate chelation in Me*p*dG (**1**) could, however, affect its N $\rightleftharpoons$ S pseudorotational equilibrium and result in higher conformational purity. On the other hand, the interaction of Zn^{2+} ions with the 3′-phosphodiester group in dG*p*Me (**2**) changes the strength of the [O4′−C4′−C3′−O3′] *gauche* effect which should be observed through the specific shift of the N $\rightleftharpoons$ S pseudorotational equilibrium towards the S-type conformers. It is, however, clear from the $\Delta\delta$ values given in Table 1 that Zn^{2+} ions interact predominantly with N7 in dG*p*Me (**2**) which strengthens the anomeric effect and drives the N $\rightleftharpoons$ S pseudorotational equilibrium towards N-type pseudorotamers. As the [O4′−C4′−C3′−O3′] *gauche* effect and the anomeric effect counteract each other in the drive of the N $\rightleftharpoons$ S pseudorotational equilibrium, the overall increase in the population of N-type pseudorotamers is larger in Me*p*dG (**1**) than in dG*p*Me (**2**).

The ^{1}H-NMR chemical shift changes of the H8, H1′ and H2′ resonances for Me*p*dG (**1**) at seven concentrations in the range from 60 mM to 1 mM afforded the average association constant ($K_{av} = 3.5 \pm 1.6$ M^{-1}) which suggested the presence of 94% (±3) of unstacked molecules at a 10 mM concentration. Similar evaluation of self-association of Me*p*dG (**1**) after titration with Mg^{2+} ions ($R = 1.0$) with the use of the chemical shift changes of the H8, H1′, H2′ and H2″ signals gave a K_{av} value of 3.0 ± 1.5 M^{-1} corresponding to 94% (±3) of unstacked molecules at a 10 mM concentration. The interpretation of the chemical shifts of

Table 3. The comparative effect of metal ions on the N ⇌ S pseudorotational equilibrium of Me*p*dG (**1**) and dG*p*Me (**2**)[a]

Metal	*R*	P_N	$\Psi_m{}^N$	P_S	$\Psi_m{}^S$	% S_{free}	% $S_M{}^{2+}$	ΔJ_{max}	r.m.s.
				Me*p*dG (**1**)					
M^{2+}-free	0.0	−23.2	37.5	163.9	37.5	67.7	–	0.43	0.202
Mg^{2+}	2.0	−22.0	37.3	164.9	37.3	67.9	67.4	0.45	0.189
Zn^{2+}	2.0	−26.4	37.6	166.5	37.6	67.4	62.4	0.50	0.232
Hg^{2+}	0.2	−28.4	37.6	165.4	37.6	67.1	66.6	0.45	0.215
				dG*p*Me (**2**)					
Metal	*R*	P_N	$\Psi_m{}^N$	P_S	$\Psi_m{}^S$	% S_{free}	% $S_M{}^{2+}$	ΔJ_{max}	r.m.s.
M^{2+}-free	0.0	−32.1	38.2	162.0	38.2	74.6	–	0.32	0.276
Mg^{2+}	2.0	−30.5	38.1	161.5	38.2	74.7	74.5	0.31	0.282
Zn^{2+}	2.0	−26.9	37.7	163.0	37.6	75.1	72.0	0.38	0.304
Hg^{2+}	0.2	−32.0	38.1	163.5	38.1	74.7	73.3	0.36	0.274

[a] Phase angle of pseudorotation and maximum puckering amplitude for N-(P_N and $\Psi_m{}^N$) and S-type (P_S and $\Psi_m{}^S$) pseudorotamers are in degrees, root-mean-square error (r.m.s.) and the maximum individual discrepancy between experimental and calculated coupling constants (ΔJ_{max}) are in Hz.

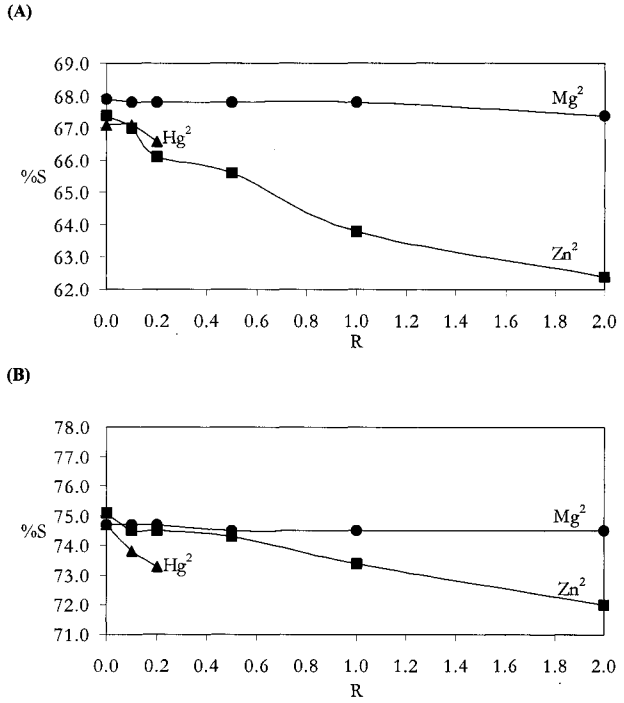

Figure 3. The N ⇌ S pseudorotational equilibrium in Me*p*dG (**1**) (panel A) and dG*p*Me (**2**) (panel B) as a function of increasing metal ion concentration

the H8, H2′ and H2″ signals in Me*p*dG (**1**) in the presence of Zn^{2+} ions (R = 1.0) resulted in a K_{av} value of 27.2 ± 17.0 M^{-1} which corresponds to 67% (± 14) of unstacked species at a 10 mM concentration of Me*p*dG (**1**). The additional titration of Me*p*dG (**1**) with Zn^{2+} ions from R = 0.0 to R = 2.0 was performed at a 1 mM concentration, where 95% (±3) of species was found to be unstacked. The comparison of the results at the two concentrations showed that the geometries of both major and minor conformers and their respective populations differed only slightly (for 1 mM: P_N = −24.9°, $\Psi_m{}^N$ = 37.4°, P_S = 165.3°, $\Psi_m{}^S$ = 37.4°,%S_{free} = 68.1 and %$S_{Zn^{2+}}$ = 65.5 at R = 2.0, r.m.s. error = 0.217 Hz, ΔJ_{max} = 0.4 Hz; for 10 mM see Table 3). Although the fraction of unstacked species decreases from 95% at 1 mM to 67% at 10 mM concentration, the Zn^{2+}-promoted drive of the N ⇌ S pseudorotational equilibrium towards N changes by only 2 percentage points which is within the error limits. There is therefore a definite M^{2+}-promoted drive of the N ⇌ S pseudorotational equilibrium towards N which is not affected considerably by the extent of self-association and the conclusions on the tuning of the N ⇌ S equilibrium by M^{2+} interactions with N7 of the nucleobase at a 10 mM concentration remain unchanged.

The comparison of the temperature-dependent shift of the N ⇌ S pseudorotational equilibrium from 278 K to 338 K at 1 and 10 mM Me*p*dG (**1**) upon interaction with Zn^{2+} (R = 1.0) has shown the following: (i) the geometries of the interconverting N and S conformers are nearly identical [for 1 mM: (P_N = −28.0°, $\Psi_m{}^N$ = 37.5°) ⇌ (P_S = 166.0°, $\Psi_m{}^S$ = 37.5°); for 10 mM: (P_N = −25.2°, $\Psi_m{}^N$ = 37.3°) ⇌ (P_S = 166.5°, $\Psi_m{}^S$ = 37.3°)], and (ii) the decrease in the population of S-type pseudorotamers with the increase of temperature is smaller at a 10 mM than at a 1 mM concentration (for 1 mM: $\%S^{278K}$ = 68.5, $\%S^{338K}$ = 64.0 and for 10 mM: $\%S^{278K}$ = 66.8, $\%S^{338K}$ = 63.8). The increase in temperature from 278 K to 338 K caused the upfield shift of the H8 signal from δ = 8.125 to δ = 8.069 at 10 mM, and from δ = 8.097 to δ = 8.043 at 1 mM Me*p*dG (**1**). The ^{1}H-NMR Δδ values between 278K and 338K are indeed very similar for all resonances at 1 and 10 mM Me*p*dG (**1**). The shift of the N ⇌ S pseudorotational equilibrium is slightly different, which indicates that as more nucleotide becomes unstacked with the increase of temperature, the Zn^{2+}-promoted drive towards N-type sugar conformation becomes comparable at the two concentrations. The temperature-dependent population changes, however, do not allow us to dissect the effect of enthalpy and entropy contributions to the Zn^{2+}-promoted drive towards N-type sugar conformation from the drive of the

N ⟷ S equilibrium due to the variation of the stability constant of labile M^{2+}−nucleotide species with temperature.

syn ⟷ *anti* Equilibrium

The semiquantitative information about the conformational equilibrium across the glycosyl bond (χ) in Me*p*dG (**1**) and dG*p*Me (**2**) upon the interactions with metal ions has been calculated from H8 ↔ H1′ NOEs.[32] Me*p*dG (**1**) showed a preference of 62% for *anti* conformation, whereas dG*p*Me (**2**) showed a preference of 69% for *syn* conformation (Figure 4). The higher tendency for *anti* conformation in Me*p*dG (**1**) relative to that in dG*p*Me (**2**) can be explained by the unfavorable steric interactions between the 5′-phosphodiester group and the nucleobase which are both on the β side in Me*p*dG (**1**). The binding of divalent metal ions to Me*p*dG (**1**) and dG*p*Me (**2**) caused a shift of the *syn* ⟷ *anti* equilibrium towards *anti*, except in the case of Mg^{2+} interactions with dG*p*Me (**2**) which caused a slight shift of 2 percentage points (within experimental error) towards *syn* (Figure 4). The steric bulk of the phosphate group on the β side of the furanosyl moiety in Me*p*dG (**1**) increases with the (electrostatic) interaction of Mg^{2+} ions with the phosphate oxygen atoms, which forces the nucleobase to adopt an *anti* conformation where the steric hindrance is reduced.

It is interesting to note that the shift of the *syn* ⟷ *anti* equilibrium in both Me*p*dG (**1**) and dG*p*Me (**2**) towards *anti* upon binding of Zn^{2+} ions is correlated with the increased population of N-type pseudorotamers. Similar correlations have already been reported.[16,33]

Conformational Equilibrium Across the C4′−C5′ Bond (γ)

The isochronicity of H5′ and H5′′ in Me*p*dG (**1**) prevented the measurement of individual $^3J_{4'5'}$ and $^3J_{4'5''}$ coupling constants. Analysis of the experimental $^3J_{4'5'}$ and $^3J_{4'5''}$ coupling constants (Table 2) in dG*p*Me (**2**) has shown 56% population of γ^+, 28% of γ^t and 16% of γ^- rotamers. Note, that the small changes in the experimental $^3J_{4'5'}$ and $^3J_{4'5''}$ coupling constants of 0.1 Hz (Table 2) upon interaction of M^{2+} ions with dG*p*Me (**2**) indicate negligible redistribution of the conformational equilibrium across γ.

Conformational Equilibrium Across the C5′−O5′ (β) and C3′−O3′ (ε) Bonds

The conformational equilibrium across the torsion angle β[C4′−C5′−O5′−P] has been assessed on the basis of experimental $^3J_{C4'P}$ coupling constants[34] alone as the isochronicity of H5′ and H5′′ protons in Me*p*dG (**1**) prevented the determination of the individual $^3J_{H5'P}$ and $^3J_{H5''P}$ coupling constants. It turned out that β^t conformers are preferred by 76.7% in M^{2+}-free solution of Me*p*dG (**1**). The

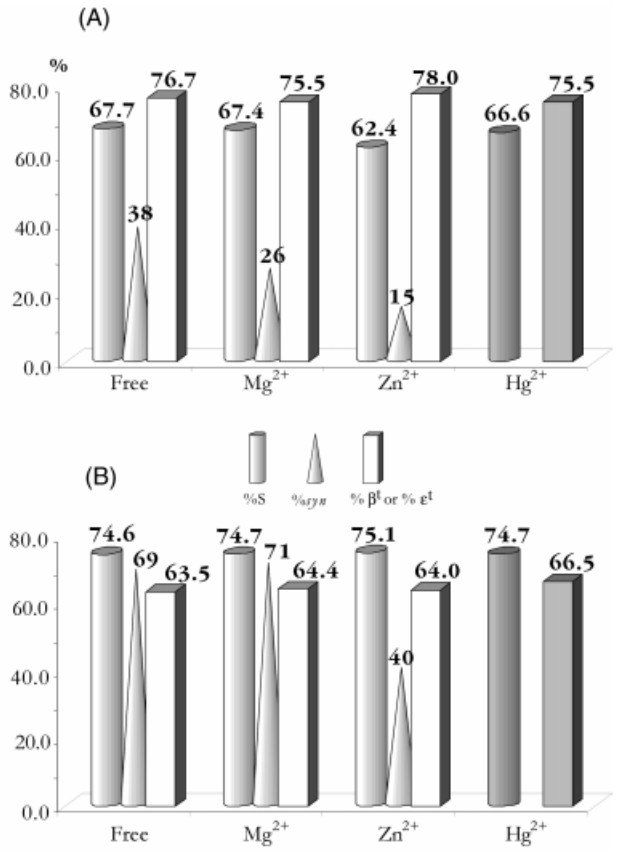

Figure 4. Changes in the conformational equilibria upon interaction of Mg^{2+}, Zn^{2+} and Hg^{2+} ions with Me*p*dG (**1**) (panel A) and dG*p*Me (**2**) (panel B); the population of S-type conformers (% S) is represented with cylinders, population of *syn* conformers (% *syn*) with cones, and population of β^t rotamers (% β^t) in Me*p*dG (**1**) and ε^t rotamers (% ε^t) in dG*p*Me (**2**) with square blocks; note that different levels of shading illustrate that data for Mg^{2+} and Zn^{2+} correspond to the addition of two molar equivalents ($R = 2.0$) of metal ions, whereas data for Hg^{2+} ions correspond to $R = 0.2$

increase in metal ion concentration showed only small changes of ca. 1 percentage point in β^t population, which is well within the range of experimental error (Table 4), and suggests that the conformation along the torsion angle β is not affected by metal ion binding to Me*p*dG (**1**).

Table 4. The effect of metal ions on the conformational equilibria across the C5′−O5′ bond (β torsion) in Me*p*dG (**1**) and across the C3′−O3′ bond (ε torsion)[a] in dG*p*Me (**2**)

	Me*p*dG (**1**)			dG*p*Me (**2**)		
	% β^t	ε^t	ε^-	% ε^t	ΔJ_{max}	r.m.s.
M^{2+}-free	76.7	209.5	270.8	63.5	0.44	0.39
Mg^{2+}	75.5	209.0	270.9	64.4	0.29	0.31
Zn^{2+}	78.0	209.4	270.7	64.0	0.81	0.52
Hg^{2+}	75.5	209.6	270.7	66.5	0.53	0.42

[a] Torsion angles ε^t and ε^- are in degrees, root-mean-square error (r.m.s.) and maximum discrepancy between the experimental and calculated $^3J_{C4'P}$, $^3J_{C2'P}$ and $^3J_{H3'P}$ coupling constants (ΔJ_{max}) are in Hz.

The experimental $^3J_{H3'P}$, $^3J_{C4'P}$ and $^3J_{C2'P}$ coupling constants (Table 2) have been used for the determination of the conformational equilibrium across the C3′−O3′ bond

(torsion angle ε[C4′−C3′−O3′−P]) in dG*p*Me (**2**) in terms of a two-state $\varepsilon^t \rightleftharpoons \varepsilon^-$ conformational equilibrium.[35−38] The ε^t rotamer is preferred by 63.5% in M^{2+}-free dG*p*Me (**2**) (Table 4). Interaction of hard Mg^{2+} and softer Zn^{2+} or Hg^{2+} ions with dG*p*Me (**2**) resulted in the minor increase (< 3 percentage points) in the preference for ε^t conformers which is not correlated with the relatively higher affinity of Mg^{2+} ions for the interaction with phosphate oxygen atoms (Table 4). Additionally, $^4J_{H2'P}$ coupling constants have been used for the qualitative assessment of the population of ε^- rotamers[39] and the results from both methods are in nice agreement (Table 4).

Conclusions

Me*p*dG (**1**) and dG*p*Me (**2**), which consist of all three structural elements of single-stranded DNA, have been chosen as simple model compounds for the evaluation of metal ion binding sites and related conformational changes in the absence of intermolecular interactions. The metal ion concentrations have been gradually increased by titration of aqueous solutions of Me*p*dG (**1**) and dG*p*Me (**2**). Multinuclear ^{1}H-, ^{13}C-, ^{15}N- and ^{31}P-NMR spectroscopy has been used to evaluate all rotational degrees of freedom across the sugar-phosphate backbone and glycosyl torsion angles.

The chemical shift changes showed that hard Mg^{2+} ions interact preferentially with the phosphate oxygen atoms in Me*p*dG (**1**), whereas in the case of dG*p*Me (**2**) the interaction of Mg^{2+} ions with the phosphate oxygen atoms competes with the interaction to the C6=O carbonyl group. Softer Zn^{2+} and Hg^{2+} ions were found to show a strong binding affinity for N7 in both Me*p*dG (**1**) and dG*p*Me (**2**).

The interpretation of $^3J_{HH}$ coupling constants in Me*p*dG (**1**) and dG*p*Me (**2**) has shown the bias of their N $\rightleftharpoons$ S pseudorotational equilibria towards S-type conformers. At 298 K the population of C2′-*endo* pseudorotamers in M^{2+}-free aqueous solutions of Me*p*dG (**1**) and dG*p*Me (**2**) were 68% and 75%, respectively. Titration of Me*p*dG (**1**) and dG*p*Me (**2**) with Mg^{2+} ions caused no observable changes in the N $\rightleftharpoons$ S pseudorotational equilibrium. On the other hand, the interaction of Zn^{2+} and Hg^{2+} ions with N7 strengthens the anomeric effect which is apparent from the increase in the population of N-type pseudorotamers. The shift of the N $\rightleftharpoons$ S pseudorotational equilibrium towards N-type conformers upon addition of two molar equivalents of Zn^{2+} was 5 percentage points for Me*p*dG (**1**) and 3 percentage points for dG*p*Me (**2**). The changes in the N $\rightleftharpoons$ S pseudorotational equilibrium are small compared to the changes caused by protonation which can be explained by the solvation of metal ions with water molecules, which mediate the interaction and thus reduce the effect of labile metal ion interaction on the redistribution of π-electron density of the guanine residue in Me*p*dG (**1**) and dG*p*Me (**2**).

The binding of divalent metal ions to Me*p*dG (**1**) and dG*p*Me (**2**) causes a shift of the *syn* $\rightleftharpoons$ *anti* equilibrium towards *anti*, which is larger for softer Zn^{2+} than harder Mg^{2+} ions. The increase in the population of *anti* conformers in both Me*p*dG (**1**) and dG*p*Me (**2**) upon binding of Zn^{2+} ions is correlated with the increased population of N-type pseudorotamers.

The small changes in the experimental $^3J_{4'5'}$ and $^3J_{4'5''}$ coupling constants in dG*p*Me (**2**) upon interaction with M^{2+} ions indicate negligible redistribution of the conformational equilibrium across C4′−C5′ bond (γ torsion).

The interpretation of $^3J_{C4'P}$ coupling constant has shown that β^t conformers are preferred by ca. 77% in M^{2+}-free aqueous solution of Me*p*dG (**1**). Only small changes of ca. 1 percentage point in the β^t population have been found upon metal ion binding to Me*p*dG (**1**).

The two-state $\varepsilon^t \rightleftharpoons \varepsilon^-$ conformational equilibrium is biased towards ε^t rotamers by 63.5% in dG*p*Me (**2**). The interaction of hard Mg^{2+} and softer Zn^{2+} or Hg^{2+} ions with dG*p*Me (**2**) resulted in the minor increase below 3 percentage points in the population of ε^t conformers.

Experimental Section

Synthesis: The synthesis of Me*p*dG (**1**) and dG*p*Me (**2**) has been carried out by procedures reported by Khorana[48,49] and Marzilli.[20] 2′-Deoxyguanosine-3′-monophosphate and 2′-deoxyguanosine-5′-monophosphate have been suspended in dry methanol. After addition of three molar equivalents of dicyclohexylcarbodiimide (DCC), the suspension was stirred at room temperature for 72 h. The solvent was evaporated under reduced pressure and water was added to precipitate DCC and its byproducts. The filtrate was extracted with petroleum ether and water removed by lyophilization.

NMR Measurements: ^{1}H- and ^{31}P-NMR spectra were recorded with a Varian Unity-plus 300 at 299.858 MHz and at 121.384 MHz, respectively. ^{13}C- and ^{15}N-NMR were acquired at 150.909 MHz and 60.817 MHz, respecitvely, with a Varian Unity Inova 600 NMR spectrometer at the National NMR Center of Slovenia. Spectra were acquired in D_2O (99.9% deuterium) at neutral pH (pH* = 7.5) at a 10 mM concentration, which is a compromise between the extent of self-association and the sensitivity of NMR measurements of rare nuclei like ^{15}N. Trimethylsilylpropionic acid was used as internal standard for ^{1}H- and ^{13}C-NMR (δ = 0) spectra, MeCN (δ = −135.8) as external reference for ^{15}N-NMR spectra, and 85% aq. H_3PO_4 (δ = 0) as external reference for ^{31}P-NMR spectra. The sample temperature was 298K ± 0.5K. Metal ion concentration was gradually increased by simple titration of nucleotides with 0.1, 0.2, 0.5, 1.0 and 2.0 molar equivalents of nitrate salts of Mg^{2+}, Zn^{2+} and Hg^{2+} ions. 1D-^{1}H measurements were performed under identical spectral and processing conditions: 9 ppm sweep width, 32K time domain, zero filling to 128K, and slight Gaussian apodization to give enhanced resolution. In order to obtain accurate *J* coupling data and chemical shifts ^{1}H-NMR spectra were simulated with a standard computer simulation algorithm, which is integrated into the Varian software package (VNMR rev. 5.3B).[28] The error in $^3J_{HH}$ is 0.1 Hz as estimated from the comparison of the experimental and simulated spectra. 1D-NOE experiments were run with 5 s irradiation time and with saturation of individual lines within the multiplet. NOE difference spectra were obtained by internal subtraction of on- and off-resonance spectra. Proton-decoupled ^{13}C-NMR spectra were recorded with 220 ppm sweep, 96K time domain, zero filling to 512K. Proton-

decoupled ^{31}P-NMR spectra were acquired with 100 ppm sweep, 56K time domain, zero filling to 64K. ^{15}N-NMR chemical shifts were obtained from 2D-HMBC experiments using gradients for coherence selection; 4096 (ω2) × 128 (ω1) data points, 320 scans per FID, 16 dummy scans, appropriate delays were calculated according to $^{1}J_{NH}$ = 90 Hz and $^{n}J_{NH}$ = 4 Hz, 6 kHz (ω2) × 15 kHz (ω1) spectral width, transformed after multiplication with a sine bell filter shifted by π/2 in both ω2 and ω1 to give an 8K × 1K matrix. Digital resolutions were 0.05 Hz in ^{1}H-NMR spectra, 0.1 Hz in ^{13}C-NMR spectra, 0.3 Hz in ^{31}P-NMR spectra and 30 Hz along the ^{15}N(*f*1) axis of 2D-HMBC spectra. − The chemical shift measurements at seven concentrations in the range from 60 mM (solubility limit) to 1 mM were employed to study self association with the isodesmic model.[53] In this model, the assumption is made that all the equilibrium constants for the $N_n + N \rightleftarrows N_{n+1}$ equilibria are equal. The observed chemical shift (δ_{obs}) is defined by Equation 1 where *c* is the total concentration of a nucleotide, δ_0 represents the chemical shift at infinite dilution, δ_∞ is the chemical shift at infinitely long stack, and *K* is the association constant.

$$\delta_{obs} = \delta_\infty + \frac{(\delta_\infty - \delta_0)\cdot(1-\sqrt{4Kc+1})}{2Kc} \quad (1)$$

Conformational Analysis: The conformational analysis of the sugar moiety was performed by the computer program PSEUROT[31] with the use of λ electronegativities for the substituents along H−C−C−H fragments and the six-parameter set from 1994 for the generalized Karplus-type equation.[29] The following λ electronegativity values were used: 0.0 for H, 0.58 for heterocycle, 1.26 for OH, 0.62 for C1′, C3′ and C4′, 0.74 for C2′, 1.27 for O4′ and 0.68 for C5′. The analysis of $^{3}J_{HH}$ coupling constants consists of three standard translation steps. First step translates experimental proton−proton coupling constants to proton-proton torsion angles and is covered by the generalized Karplus−Altona equation. Second step is the translation of proton−proton torsion angles into the corresponding endocyclic torsion angles and is formulated with the set of linear equations $\Phi_{HH} = A\nu_j + B$. Φ_{HH} is the torsion angle between two vicinal protons and ν_j is the corresponding endocyclic torsion angle. Parameters A and B were determined from a large collection of X-ray data. Third translational step of endocyclic torsion angles into the pseudorotational parameters is described by a simple cosine function $\nu_j = \Psi_m \cdot \cos[P + (j - 2) \cdot 4\pi/5]$, where *P* is the phase angle of pseudorotation and Ψ_m is the maximum puckering amplitude. In the following optimization procedure the geometries and populations of N and S pseudorotamers are varied to obtain the best fit between experimental and calculated coupling constants. Our optimization procedure was started with the following input values: P_N = 18°, $\Psi_m{}^N$ = 36°, P_S = 156°, $\Psi_m{}^S$ = 36°. The puckering amplitude of the minor N conformer ($\Psi_m{}^N$) was kept frozen during individual iterative least-squares optimization, while all other parameters were freely optimized. The best fits are given in Table 3 together with error evaluation in terms of maximum individual Δ*J* and root-mean-square error. − The population of the β^t rotamers was calculated with the following equation: $x_{\beta t} = [^3J_{C4'P}(expt) - {}^3J_{C4'P}(60°)]/[^3J_{C4'P}(180°) - {}^3J_{C4'P}(60°)] = (^3J_{PC4'}(expt) - 0.7)/10.3$, where the values of 11.0 Hz and 0.7 Hz have been used as the limiting coupling constants for $^3J_{C4'P}(180°)$ and $^3J_{C4'P}(60°)$, respectively.[34] − The population across the C4′−C5′ bond was evaluated on the basis of experimental $^3J_{4'5'}$ and $^3J_{4'5''}$ coupling constants which were interpreted with the assumption of the conformational equilibrium between three staggered conformers.[50] The limiting coupling constants were calculated[29] with the use of the torsion angles γ from a survey of X-ray crystallographic data (*gauche*-plus, γ = 53° ⇌ *gauche*-trans, γ = 180° ⇌ *gauche*-minus, γ = −70°).[50] The limiting coupling constants and populations of the three rotamers are related with the following equations: $^3J_{4'5'} = 1.64\ x_{\gamma+} + 2.86\ x_{\gamma t} + 10.40\ x_{\gamma-}$ and $^3J_{4'5''} = 1.84\ x_{\gamma+} + 10.78\ x_{\gamma t} + 2.71\ x_{\gamma-}$. − The interpretation of the experimental $^3J_{C4'P}$, $^3J_{C2'P}$ and $^3J_{H3'P}$ coupling constants has been performed with the assumption of a two-state $\varepsilon^t \rightleftarrows \varepsilon^-$ conformational equilibrium across the C3′−O3′ bond in dG*p*Me (**2**). The three-parameter Karplus equations[37,38] for $^3J_{CP} = 9.1 \cdot \cos^2\Phi - 1.9 \cdot \cos\Phi + 0.8$ and $^3J_{HP} = 15.3 \cdot \cos^2\Phi - 6.2 \cdot \cos\Phi + 1.5$ have been used in the calculation of $^3J_{CP}$ and $^3J_{HP}$ from ε^t and ε^- torsion angles and their respective populations, which were iterated to find the best fit with the experimental $^3J_{C4'P}$, $^3J_{C2'P}$ and $^3J_{H3'P}$ coupling constants. An additional semiquantitative estimation of the population of ε^- rotamers was done with the equation $x_{\varepsilon^-} = {}^4J_{H2'P}(expt)/2.3$,[39] which showed that population of ε^- rotamers is in the range from 30 to 35 percentage points. − The populations of *syn* and *anti* conformers could be estimated with the use of 1D-NOE difference spectroscopy by saturating H8 and measuring the NOE at H1′ for *syn*, and the sum of NOEs at H2′ and H3′ for the *anti* conformers.[32] As the signal for H3′ is overlapping with the signal of residual HOD for both Me*p*dG (**1**) and dG*p*Me (**2**) and its suppresion could introduce considerable error in our evaluation of *syn* ⇌ *anti* equilibrium we have only used H8 ↔ H1′ NOEs. Nuclear Overhauser enhancements upon saturation of H8 were 4.3% and 7.8% for free Me*p*dG (**1**) and dG*p*Me (**2**), respectively, 2.9% and 8.1% for Mg^{2+} (*R* = 2.0) and 1.7% and 4.5% for Zn^{2+} (*R* = 2.0). The NOE enhancements were used to calculate the population of *syn* conformers with the following equation: %*syn* = 100 · ηH1′/11.3.[32]

Acknowledgments

We thank the Ministry of Science and Technology of Republic of Slovenia (Grant No. Z1−8609−0104) and Krka, Pharmaceutical and Chemical Works, Novo mesto, Slovenia for the financial support and for their financial contribution for the purchase of 300- and 600-MHz Varian NMR spectrometers.

[1] For a recent review on the studies of metal ion interactions with nucleic acid constituents see: "Interactions of Metal Ions with Nucleotides, Nucleic Acids, and Their Constituents", in *Metal Ions in Biological Systems* (Eds.: A. Sigel, H. Sigel), vol. 32, M. Dekker, New York, **1996**, pp. 814.
[2] R. M. Smith, A. E. Martell, Y. Chen, *Pure Appl. Chem.* **1991**, *63*, 1015−1080.
[3] J. E. Kilpatrick, K. S. Pitzer, R. Spitzer, *J. Am. Chem. Soc.* **1947**, *69*, 2483−2488.
[4] C. Altona, M. Sundaralingam, *J. Am. Chem. Soc.* **1972**, *94*, 8205−8212.
[5] C. Altona, M. Sundaralingam, *J. Am. Chem. Soc.* **1973**, *95*, 2333−2344.
[6] H. P. M. de Leeuw, C. A. G. Haasnoot, C. Altona, *Isr. J. Chem.* **1980**, *20*, 108−126.
[7] J. Plavec, W. Tong, J. Chattopadhyaya, *J. Am. Chem. Soc.* **1993**, *115*, 9734−9746.
[8] J. Plavec, C. Thibaudeau, G. Viswanadham, C. Sund, J. Chattopadhyaya, *J. Chem. Soc., Chem. Commun.* **1994**, 781−783.
[9] J. Plavec, L. H. Koole, J. Chattopadhyaya, *J. Biochem. Biophys. Methods* **1992**, *25*, 253−272.
[10] C. Thibaudeau, J. Plavec, K. A. Watanabe, J. Chattopadhyaya, *J. Chem. Soc., Chem. Commun.* **1994**, 537−540.
[11] C. Thibaudeau, J. Plavec, J. Chattopadhyaya, *J. Am. Chem. Soc.* **1994**, *116*, 8033−8037.
[12] C. Thibaudeau, J. Plavec, J. Chattopadhyaya, *J. Org. Chem.* **1996**, *61*, 266−286.
[13] I. Luyten, C. Thibaudeau, J. Chattopadhyaya, *J. Org. Chem.* **1997**, *62*, 8800−8808.

[14] I. Luyten, C. Thibaudeau, A. Sandström, J. Chattopadhyaya, *Tetrahedron* **1997**, *53*, 6433−6464.
[15] M. Polak, B. Mohar, J. Kobe, J. Plavec, *J. Am. Chem. Soc.* **1998**, *120*, 2508−2513.
[16] C. Thibaudeau, A. Foldesi, J. Chattopadhyaya, *Tetrahedron* **1997**, *53*, 14043−14072.
[17] M. Polak, J. Plavec, *Nucleosides Nucleotides* **1998**, *17*, 2011−2020.
[18] L. G. Marzilli, B. de Castro, C. Solorzano, *J. Am. Chem. Soc.* **1982**, *104*, 461−466.
[19] T. Theophanides, M. Polissiou, *Inorg. Chim. Acta* **1981**, *56*, L1-L3.
[20] S. K. Miller, D. G. VanDerveer, L. G. Marzilli, *J. Am. Chem. Soc.* **1985**, *107*, 1048−1055.
[21] M. D. Reily, L. G. Marzilli, *J. Am. Chem. Soc.* **1986**, *108*, 8299−8300.
[22] E. Alessio, Y. Xu, S. Cauci, G. Mestroni, F. Quadrifoglio, P. Viglino, L. G. Marzilli, *J. Am. Chem. Soc.* **1989**, *111*, 7068−7071.
[23] M. C. F. Magalhaes, S. S. Massoud, N. A. Corfu, H. Sigel, *J. Inorg. Biochem.* **1989**, *36*, 295−295.
[24] H. Sigel, S. S. Massoud, N. A. Corfu, *J. Am. Chem. Soc.* **1994**, *116*, 2958−2971.
[25] H. Sigel, *Chem. Soc. Rev.* **1993**, *22*, 255−267.
[26] The generalized all-atom AMBER force-field parameters[51] as implemented in the computer program InsightII[52] has been used to perform a simple energy minimization of dGpMe (**2**). The starting conformation was built in such a way that it agrees with our NMR-derived conformational preferences: South sugar coformation, γ^+, ε^t, *anti*. The distances between N7 and phosphate oxygen atoms in the energy-minimized conformer ($P = 148°$, $\Psi_m = 39°$, $\gamma = 67°$, $\varepsilon = 187°$, $\chi = 244°$) were: 6.54, 6.81, 7.85 and 8.70 Å.
[27] D. G. Gorenstein, *Chem. Rev.* **1994**, *94*, 1315−1338.
[28] *VNMR*™ data acquisition and processing software, Revision 5.3B, Varian, Palo Alto, **1997**.
[29] C. Altona, R. Francke, R. de Haan, J. H. Ippel, G. J. Daalmans, A. J. A. Westra Hoekzema, J. van Wijk, *Magn. Reson. Chem.* **1994**, *32*, 670−678.
[30] C. A. G. Haasnoot, F. A. A. M. de Leeuw, C. Altona, *Tetrahedron* **1980**, *36*, 2783−2792.
[31] F. A. A. M. de Leeuw, C. Altona, *J. Comput. Chem.* **1983**, *4*, 428−437.
[32] H. Rosemeyer, G. Toth, B. Golankiewicz, Z. Kazimierczuk, W. Bourgeois, U. Kretschmer, H.-P. Muth, F. Seela, *J. Org. Chem.* **1990**, *55*, 5784−5790.
[33] W. Saenger Principles of Nucleic Acid Structure (Ed.: C. R. Cantor), Springer Verlag, New York, **1984**.
[34] P. P. Lankhorst, C. A. G. Haasnoot, C. Erkelens, C. Altona, *J. Biomol. Struct. Dyn.* **1984**, *1*, 1387−1405.
[35] P. P. Lankhorst, C. A. G. Haasnoot, C. Erkelens, H. P. Westerink, G. A. van der Marel, J. H. van Boom, C. Altona, *Nucleic Acids Res.* **1985**, *13*, 927−942.
[36] J. Plavec, C. Thibaudeau, G. Viswanadham, A. Sandstöm, J. Chattopadhyaya, *Tetrahedron* **1995**, *51*, 11775−11792.
[37] J. Plavec, J. Chattopadhyaya, *Tetrahedron Lett.* **1995**, *36*, 1949−1952.
[38] M. M. W. Mooren, S. S. Wijmenga, G. A. van der Marel, J. H. van Boom, C. W. Hilbers, *Nucleic Acids Res.* **1994**, *22*, 2658−2666.
[39] M. J. J. Blommers, D. Nanz, O. Zerbe, *J. Biomol. NMR* **1994**, *4*, 595−601.
[40] D. P. Bancroft, C. A. Lepre, S. J. Lippard, *J. Am. Chem. Soc.* **1990**, *112*, 6860−6871.
[41] D. Yang, S. S. G. E. van Boom, J. Reedijk, J. H. van Boom, A. H.-J. Wang, *Biochemistry* **1995**, *34*, 12912−12920.
[42] F. Reeder, F. Gonnet, J. Kozelka, J. C. Chottard, *Chem. Eur. J.* **1996**, *2*, 1068−1076.
[43] J. Kasparkova, K. J. Mellish, Y. Qu, V. Brabec, N. Farrell, *Biochemistry* **1996**, *35*, 16705−16713.
[44] G. Admiraal, M. Alink, C. Altona, F. J. Dijt, C. J. van Garderen, R. A. G. de Graaf, J. Reedijk, *J. Am. Chem. Soc.* **1992**, *114*, 930−938.
[45] F. Reeder, Z. J. Guo, P. D. Murdoch, A. Corazza, T. W. Hambley, S. J. Berners-Price, J. C. Chottard, P. J. Sadler, *Eur. J. Biochem.* **1997**, *249*, 370−382.
[46] M. Iwamoto, S. Mukundan, L. G. Marzilli, *J. Am. Chem. Soc.* **1994**, *116*, 6238−6244.
[47] M. J. Bloemink, E. L. M. Lempers, J. Reedijk, *Inorg. Chim. Acta* **1990**, *176*, 317−320.
[48] H. G. Khorana, *J. Am. Chem. Soc.* **1959**, *81*, 4657−4660.
[49] M. Smith, J. G. Moffatt, H. G. Khorana, *J. Am. Chem. Soc.* **1958**, *80*, 6204−6212.
[50] C. A. G. Haasnoot, F. A. A. M. de Leeuw, H. P. M. de Leeuw, C. Altona, *Recl. Trav. Chim. Pays-Bas* **1979**, *98*, 576−577.
[51] S. J. Weiner, P. A. Kollman, D. T. Nguyen, D. A. Case, *J. Comput. Chem.* **1986**, *7*, 230−252.
[52] *Insight II*, BIOSYM/Molecular Simulations, San Diego, CA, **1995**.
[53] R. B. Martin, *Chem. Rev.* **1996**, *96*, 3043−3064.

Received April 28, 1998
[I98265]